Skin Cancer Detection using Neutrosophic c-means and Fuzzy c-means Clustering Algorithms

Ahmed Abdelhafeez[*1], Hoda K. Mohamed [2]

[1] Faculty of Information Systems and Computer Science, October 6th University, Cairo, 12585, Egypt
[2] Faculty of Engineering, Ain shams University, Cairo, 11566, Egypt

Emails: aahafeez.scis@o6u.edu.eg; Hoda.korashy@eng.asu.edu.eg

Abstract

Melanoma is the kind of skin cancer that poses the greatest risk to one's life and has the maximum mortality rate within the group of skin cancer disorders. Even so, the automated placement and classification of skin lesions at initial phases remains a complicated task due to the lack of contrast melanoma molarity and skin fraction and a greater level of color similarity among melanoma-affected and -nonaffected areas. Contemporary technological improvements and research methods enabled it to recognize and distinguish this type of skin cancer more successfully. A clustering technique called neutrosophic c-means clustering (NCMC) is presented in this research to group ambiguous data in the detection of skin cancer. This algorithm takes its cues from both fuzzy c-means and the neutrosophic set structure. To arrive at such a structure, an appropriate objective function must first be created and then minimized. The clustering issue must then be stated as a restricted minimization problem, the solution of which is determined by the objective function. This paper made a comparison between NCMC and fuzzy c-means clustering (FCMC). The results show that the NCMC is more suitable than the FCMC.

Keywords: Skin cancer; Neutrosophic set; Clustering; Neutrosophic c-means clustering; Fuzzy c-means clustering

1. Introduction

Tumour is a kind of skin cancer that may be lethal, and each year it is responsible for the deaths of thousands of individuals all over the world who suffer from it. Its primary target regions are the sections of the human body that continue to be exposed to sunlight, such as the face, arms, legs, neck, and other similar locations. Melanoma has the unfortunate distinction of having the highest mortality rate of all cancers. The unexpected growth of the skin pigments forming the body cells is the major cause of melanoma[1]–[3]. The severity of the condition determines the form and color of the melanoma moles that are created, which may take on a variety of appearances including pink, red, black, brown, and so on. To rule out the possibility of melanoma infection, the dermatologist must inspect any moles that are larger than 6 millimeters in diameter and have an unusual color hue. Dermatologists will first conduct a visual examination of the behavior in question by assessing the form, size, aberrant skin color, and diameter of the moles that have been generated. However, given the limited number of dermatologists in practice today, the procedure of diagnosis may be time-consuming, which might lower a person's odds of surviving their condition[4]–[6]. However, if the sickness is identified in its early stages, then it is possible to not only save individuals from the agonizing process of undergoing biopsies, but it is also possible to boost the likelihood that a victim would survive the illness. Therefore, to address the difficulties associated with a melanoma diagnosis,

DOI: https://doi.org/10.54216/JISIoT.080103
Received: May 15, 2022 Accepted: January 23, 2023

the researchers are currently focusing their attention on the development of automated methods for the detection of this fatal disease[7]–[9].

A few different approaches have been suggested as potential methods for the automatic identification of melanoma-affected areas of the skin. First, strategies that are handmade and based on characteristics are presented to identify melanomas. However, because of differences in the scope, shape, and color of the melanoma moles, these techniques are not producing satisfactory outcomes[10]–[12]. After that, segmentation-based approaches such as edge detection and iterative selection thresholding (ISO) are incorporated into these automated systems to increase the accuracy of their detection capabilities[13]–[15]. These methods operate on what is referred to as the area of interest, which is a sectioned-off piece of melanoma (ROI). These techniques have superior performance because the pretentious section can be quickly detected if the output feature stage has placed greater attention on the malicious region. In other words, the contaminated portion can be easily identified. The primary rationale for excluding the section of the impacted region that was not affected is because including it might result in the generation of a weak feature vector, which would negatively affect the system's ability to identify anomalies. Therefore, the first stage in the process of developing an autonomous detection system for melanomas is segmentation. Though the area of involvement or thresholding-based methodologies perform exceptionally well in situations in which there is either, no variability in the image contrast, or there are lower light changes within the source images, and the picture is portraying the uniform distribution of chromaticity. However, when dealing with situations that take place in the actual world, it is very difficult, if not physically impossible, to prevent fluctuations in the pictures' lighting and chrominance. The detection accuracy of the melanoma-affected part is thus worse when using threshold-based approaches in these kinds of situations. Methods that are based on deep learning are becoming more prevalent in the medical imaging industry nowadays. To train the automatic detection system, the CNN extracts, from inside the pictures, the minute regions that include the melanoma-affected areas. The segmentation of the test pictures is carried out using these approaches using the trained model as a guide. Deep learning-based algorithms are shown improved results than handmade feature-based strategies for the identification and segmentation of melanoma. These methods can automatically generate a complex and comprehensive collection of features straight from the input pictures, and they demonstrated improved localization and identification power for areas of the skin afflicted by melanoma. In addition, techniques based on deep learning can readily find skin moles of varied sizes even when there are blurring, noise, and fluctuations in brightness, strength, and color. Therefore, these approaches can effectively cope with the challenges of handmade and clustering melanoma identification systems, and they have captured the attention of researchers who are interested in using them for the automatic empathy of skin lesions[16], [17].

Several different algorithms developed for dermoscopic segmentation. To separate the melanoma pictures, Grana et al. used an automated thresholding approach that was based on Otsu's threshold. Rubegni et al. suggested using the zero-crossings technique of a Laplacian of Gaussian (LoG) edge to divide dermoscopy pictures. This approach was offered to segment the images. The performance of the contour and edge-based approaches suffered because of the hazy borders of the lesion because of the smooth transition that existed between the lesion and the surrounding skin. Therefore, Zhou et al. identified the lesion borders by using a customized snake paradigm that was founded on region-based methodologies. Zhou et al. employed an anisotropic mean shift-based fuzzy c-means technique, while Gao et al. presented multi-resolution Markov random arenas on dermoscopic picture recognition. However, when there are varied colors or textures of skin or lesions, region-based approaches become more complicated, and they may result in over-segmentation. Because of this, Melli et al have studied numerous methods for color clustering. These algorithms include KM, median cut, FCM, and mean shift. Of these, the mean shift technique was shown to be better in terms of both specificity and sensitivity. This is because the mean shift can adjust to the characteristics of the target picture, which enabled it to create clusters that are farther apart from one another in the feature space than they would have been otherwise. The findings demonstrated that the best-acquired identified borders were 64 for the median shift, and 6 groups for KM, FCM, and the midpoint cut[18]–[20].

To cope with the unpredictability, researchers have experimented recently with several different segmentation strategies using the FS[21], [22]. The FCM algorithm may be used to divide the pictures into multiple areas by making use of the membership of the pixel values[23], [24]. This algorithm is resistant to differences in skin tone as well as the influence of shadows. When compared to Otsu's algorithm, the skin cancer categorization approach that Lee and Chen developed and executed made use of the FCM grouping and produced much better results. In addition, neutrosophic approaches, such as the NS, have been utilized to manage the indeterminacy that arises during picture processing.

DOI: https://doi.org/10.54216/JISIoT.080103
Received: May 15, 2022 Accepted: January 23, 2023

This was done so that the results are more accurate. For effective data clustering and picture segmentation, a technique known as NCMC was used to group typical data points with other data points. Guo and Sengur developed a directed procedure (mean) in the neutrosophic color picture to minimize the group indeterminacy. They then used the revised FCM approach to the N color image in the direction to segment it. Finally, the set indeterminacy was reduced. To tackle the problem of the FCM's inability to deal with unclear data, Guo and Sengur combined both the NS and FCM settings. Using the NS shift and the shearlet transform, Guo et al. devised an effective method for segmenting microscopic pictures [25], [26].

Segmentation is often an unsupervised learning method that involves the selection of either straight or indirect parameters to determine the number of groups or sectors. These constraints may be supplied directly or indirectly. To properly understand these characteristics, you must have previous information about the data included in the picture, like the number of clusters present. When doing picture segmentation, one of many standard methods that may be used to calculate any model parameters is available for use. This allows for the realistic number of clusters to be determined. Permutation testing, cross-validation, resampling, punished likelihood estimation, and identifying the knee of the error curve are some of the methods that fall under this category. In actual practice, several studies have been carried out to define the optimum number of groups. Pei et al. provided an ideal strategy for selecting the sum of groups that is predicated on the variance between the classes and the individuals within each class[27], [28].

2. Methodology

Neutrosophic set (NS) was offered as a new field of philosophy that deals with the genesis, nature, and extent of neutralities, as well as their interconnections with a variety of other ideational spectra. An item E in the neutrosophic set is analyzed in connection to its opponent, 'Anti-E,' and its neutrality, 'Neut-E,' which is neither 'E' nor 'Anti-E.' Furthermore, three memberships are used to quantify the degree to which 'E' is true, indeterminate, or false. The NS offers a great instrument to contract with indeterminacy, and it has created useful apps in a wide range of various arenas, like DBMS, linguistic web services, economic dataset detection, and new economic development and decline examination. This character is the basis for the neutrosophic theory. In addition, the literature has examples of several applications for image processing, including image de-noising, median filter, division, and color texture image analysis. These examples may be found[29], [30].

NCMC simultaneously determines every one of the data sets, the levels to which they belong to the determining cluster as well as the indeterminate cluster. While group T can be thought of as the class label to cause groups, the memberships I and F can be utilized to calculate two distinct kinds of indeterminate groups: a confusion group and an outlier group for every data set, including both. While the membership T can be thought of as the membership degree to determinant groups, the membership T can also be regarded as the membership degree to cause groups. The ambiguity group grants us the ability to think about the specific points of data that are located close to the cluster's edges, while the outlier group grants us the ability to disregard individual data points that are located a significant distance from the centers for every group. It is during the rounds of the clustering process, and not during the decision procedure, that ambiguity and outlier groups are created. The membership grades of a data set to the uncertainty and outlier class are clear, and these principles are learned through the iterative process of clustering data points. Therefore, membership functions are less susceptible to being affected by noise, and they are very closely aligned with the concept of suitability[31], [32].

FCM clustering strategy is an established scheme in the classification stage. Segmentation is amongst the most common approaches to data analysis, and it is also one of the most common procedures. In contrast to the conventional k-means method, which requires each data point to entirely conform to only one cluster, the FCM permits every data point to match two or more groups. Because of this, one of the most important steps in the clustering process is counting the number of groups present in the picture. Melanomas are significant skin lesions, and to identify them with the naked eye, you need to recognize them at an early stage so that you can tell them apart from benign skin lesions. This current study suggested a technique for skin lesion automated division that is built on a pre-determination of the number of groups' stage. The goal of this work was to tackle the challenges that arise during the manual identification of skin lesions. After that, an NCMC algorithm is used for the dermoscopy pictures to carry out the segmentation process[33], [34].

DOI: https://doi.org/10.54216/JISIoT.080103
Received: May 15, 2022 Accepted: January 23, 2023

The goal of the methods used in clustering analysis is to reduce the importance of the objective functions. The first and most basic stage in the clustering method is the specification of the goal function[35], [36].

The NS can describe each piece of data by employing the following three membership values: A, B, and C, where A refers to the level of truth, C represents the level of falsehood, and B represents the amount of indeterminacy. In the clustering method that has been presented, the letters A, B, and C are used to represent the degrees of membership to the clustering centers, the vagueness center, and the outlier center, respectively[37], [38].

The objective function can be defined as:

$$O(A,B,C,E) = \begin{pmatrix} \sum_{i=1}^{N}\sum_{j=1}^{E}(w_1 A_{ij})^m \|x_i - e_j\|^2 + \\ \sum_{i=1}^{N}\sum_{j=1}^{E_2}(w_2 B_{2ij})^m \|x_i - e_{2j}\|^2 + \\ \sum_{i=1}^{N}\sum_{j=1}^{E_3}(w_3 B_{2ij})^m \|x_i - e_{3j}\|^2 + \\ \sum_{i=1}^{N}\sum_{j=1}^{E_4}(w_4 B_{2ij})^m \|x_i - e_{4j}\|^2 + \\ \sum_{i=1}^{N}\sum_{j=1}^{E_5}(w_5 B_{2ij})^m \|x_i - e_{5j}\|^2 + \\ \sum_{i=1}^{N}\sum_{j=1}^{E_6}(w_6 B_{2ij})^m \|x_i - e_{6j}\|^2 + \\ \sum_{i=1}^{N}\sum_{j=1}^{E_7}(w_7 B_{2ij})^m \|x_i - e_{7j}\|^2 + \\ \sum_{i=1}^{N}\sum_{j=1}^{E_8}(w_8 B_{2ij})^m \|x_i - e_{8j}\|^2 + \\ \sum_{i=1}^{N}\sum_{j=1}^{E_9}(w_9 B_{2ij})^m \|x_i - e_{9j}\|^2 + \\ \dots\ \dots\ \dots\ \dots \\ \sum_{i=1}^{N}\sum_{j=1}^{E_E}(w_E B_{Eij})^m \|x_i - e_{Ej}\|^2 + \\ \sum_{i=1}^{N} J^2 (w_{e+1} C_i)^2 \end{pmatrix} \quad (1)$$

Where J refers to the number of the controlled object.

When the grouping number E is more than three, the goal function in the previous Equation becomes quite complicated, and the calculation of it takes a significant amount of time. The degree of uncertainty associated with each set of data is highly dependent on the deterministic clusters that are located nearby. In this circumstance, if we only recognize the two contiguous definite groups that have the largest and the next largest membership values, the optimization problem will be streamlined, and the data processing cost will be lowered, while the grouping precision is not be significantly decreased. This is because the biggest and the next biggest membership scores correspond to the clusters that are physically closest to one another.

The objective function can be simplified as:

$$O(A,B,C,E) = \sum_{i=1}^{N}\sum_{J=1}^{C}(w_1 A_{ij})^m \|x_i - e_j\|^2 + \sum_{i=1}^{N}(w_2 B_{ij})^m \|x_i - e_{jmax}\|^2 + \sum_{i=1}^{N} J^2 (w_3 C_i)^2 \quad (2)$$

$$e_{jmax} = \frac{E_{biggest} + E_{secondBiggest}}{2} \quad (3)$$

Where

$$\sum_{j=1}^{E} A_i + B_i + C_i = 1 \quad (4)$$

We can compute the Lagrange function as:

DOI: https://doi.org/10.54216/JISIoT.080103
Received: May 15, 2022 Accepted: January 23, 2023

$$R(A,B,C,E) = \left(\begin{array}{c} \sum_{i=1}^{N}\sum_{J=1}^{C}(w_1A_{ij})^m\|x_i-e_j\|^2 + \sum_{i=1}^{N}(w_2B_{ij})^m\|x_i-e_{jmax}\|^2 + \sum_{i=1}^{N}J^2(w_3C_i)^2 \\ -\sum_{i=1}^{N}\forall_i\left(\sum_{i=1}^{E}A_{ij}+B_i+C_i-1\right) \end{array} \right) \quad (5)$$

$$\frac{\vartheta R}{\vartheta A_{ij}} = m(w_1A_{ij})^{m-1}\|x_i-e_j\|^2 - \forall_i \quad (6)$$

$$\frac{\vartheta R}{\vartheta B_{ij}} = m(w_2B_{ij})^{m-1}\|x_i-e_{jmax}\|^2 - \forall_i \quad (7)$$

$$\frac{\vartheta R}{\vartheta C_{ij}} = J^2m(w_3C_i)^{m-1} - \forall_i \quad (8)$$

$$\frac{\vartheta R}{\vartheta E_{ij}} = -2\sum_{i=1}^{N}(w_1A_{ij})^m \quad (x_i-e_i) \quad (9)$$

$$\frac{\vartheta R}{\vartheta A_{ij}} = 0, \frac{\vartheta R}{\vartheta B_{ij}} = 0, \frac{\vartheta R}{\vartheta C_{ij}} = 0, \frac{\vartheta R}{\vartheta e_{ij}} = 0 \quad (10)$$

$$A_{ij} = \frac{1}{w_1}\left(\frac{\forall_i}{m}\right)^{1/m-1}(x_i-e_j)^{-2/m-1} \quad (11)$$

$$B_i = \frac{1}{w_2}\left(\frac{\forall_i}{m}\right)^{1/m-1}(x_i-e_{jmax})^{-2/m-1} \quad (12)$$

$$C_{ij} = \frac{1}{w_3}\left(\frac{\forall_i}{m}\right)^{1/m-1}J^{-2/m-1} \quad (13)$$

$$E_j = \frac{\sum_{i=1}^{N}(w_1A_{ij})^m x_i}{\sum_{i=1}^{N}(w_1A_{ij})^m} \quad (14)$$

Then,

$$A_{ij} = \frac{D}{w_1}(x_i-e_j)^{-2/m-1} \quad (15)$$

$$B_i = \frac{D}{w_2}(x_i-e_{jmax})^{-2/m-1} \quad (16)$$

$$C_{ij} = \frac{D}{w_3}J^{-2/m-1} \quad (17)$$

$$D = \left[\sum_{j=1}^{E}(x_i-e_j)^{-2/m-1} + (x_i-e_{jmax})^{-2/m-1} + J^{-2/m-1}\right]^{-1} \quad (18)$$

NCMC Algorithm

We can summarize the previous equations in the following steps:

Stage 1: Prepare the $A^{(0)}, B^{(0)}, and\ C^{(0)}$

Stage 2: Prepare the $E, m, \forall, w_1. w_2, w_3$

DOI: https://doi.org/10.54216/JISIoT.080103
Received: May 15, 2022 Accepted: January 23, 2023

Stage 3: For every D, we compute the value of c^e (centers)

Stage 4: Compute the value of e_{jmax} for every biggest A and the next biggest A

Stage 5: Update the value of $A^{(0)}, B^{(0)}, and\ C^{(0)}$ to the $A^{(e+1)}, B^{(e+1)}, and\ C^{(e+1)}$

Stage 6: Return to stage 3 if $\left|A^{(e+1)} - A^{(e)}\right| > \delta$ else stop

Stage: Provide the value of A, B, C to each class

3. Results

MNIST: HAM10000 and PH2 are the names of the database that was used for this study project. These are research-oriented databases that are publicly accessible to the public and each includes a collection of 10,015 and 200 dermatoscopic pictures, correspondingly. These databases are used to do an analysis and assessment of the suggested methods. To carry out this research, a sample of a whole of 500 photographs, both malignant and non-cancerous, has been obtained via the use of the HAM database. With the use of these photos, the NCMC that was presented classified 326 of the images as malignant and 174 of the images as non-cancerous. Python software is used to set up the study.

We also analyzed the clustering findings of the skin cancer database for every approach using sensitivity and specificity analysis. Sensitivity and specificity are specified in the following terms.

$$Sensitivity = \frac{True\ Positive}{True\ Positive + False\ Negative} \tag{19}$$

$$Specificity = \frac{True\ Negative}{False\ Positive + True\ Negative} \tag{20}$$

Figures 1, and 2 show the sample of the datasets.

Figures 3, and 4 show the accuracy, sensitivity, and specificity of the two datasets. In the first dataset, the accuracy equals 0.90, and in the second dataset equals 0.89. Table 1 shows the outcomes of the two datasets.

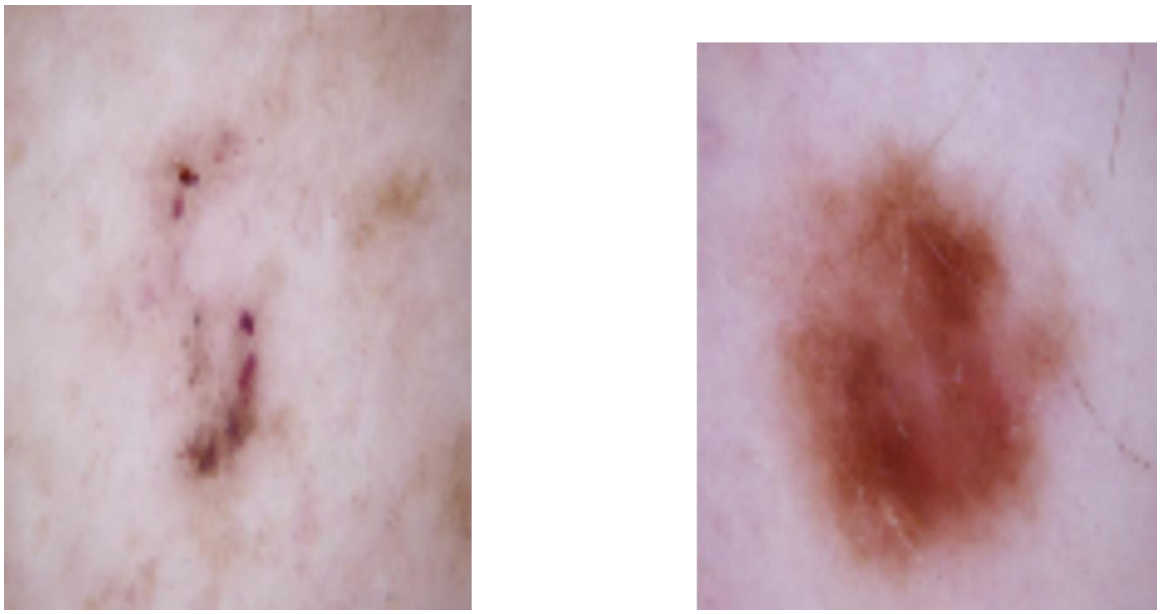

Figure 1: The patient has one disease skin cancer.

DOI: https://doi.org/10.54216/JISIoT.080103
Received: May 15, 2022 Accepted: January 23, 2023

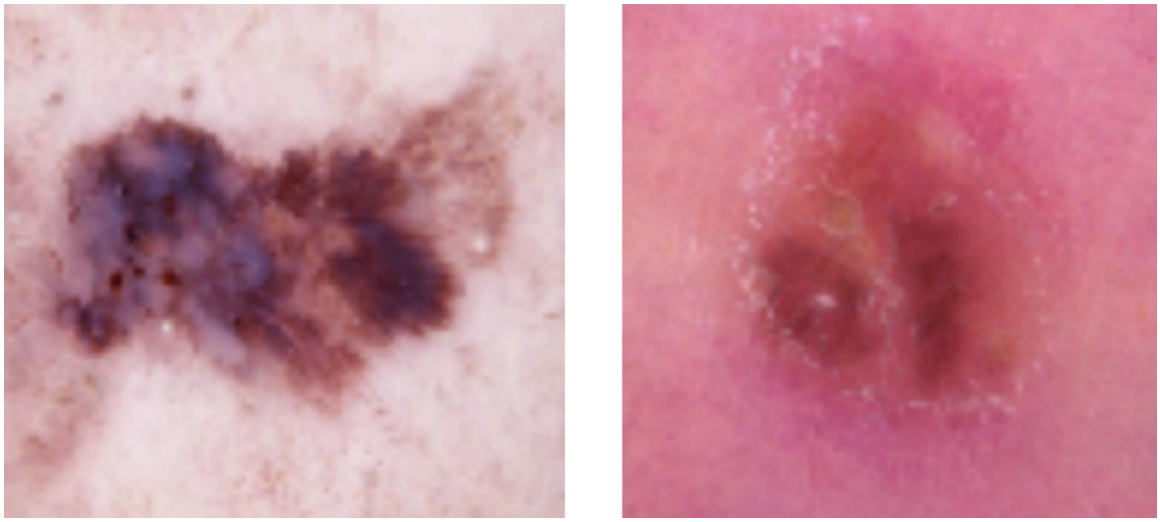

Figure 2: The patient has two diseases skin cancer.

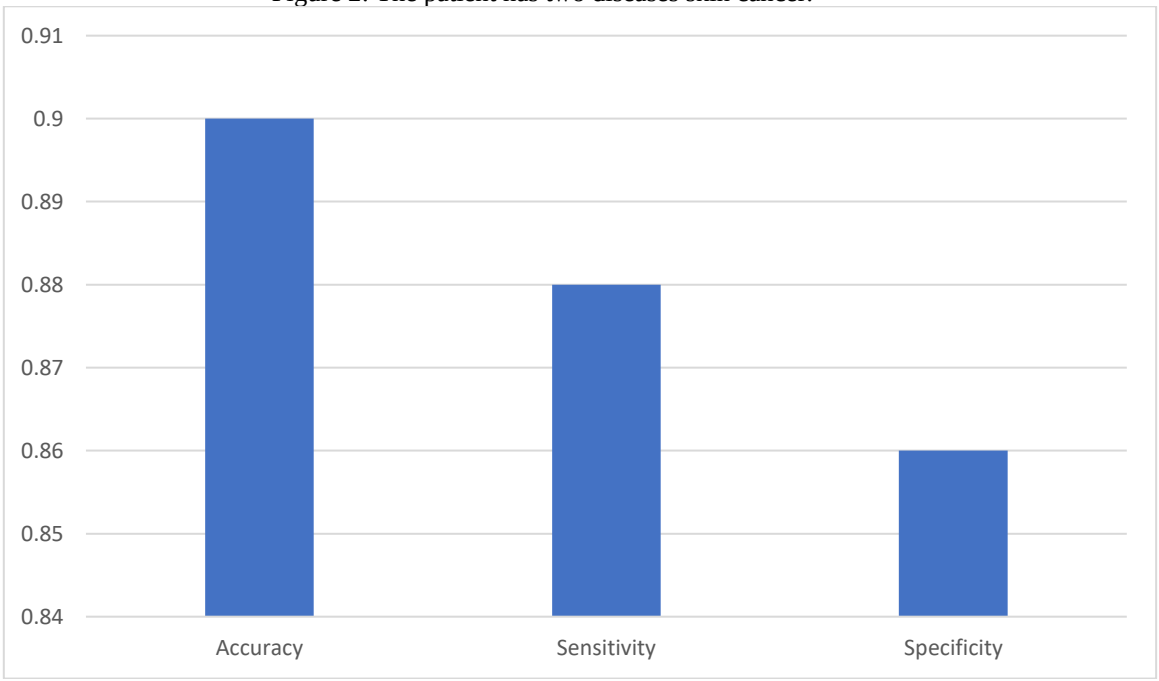

Figure 3: The accuracy of the HAM10000 dataset.

Table 1: The outcome of the two datasets

	Sensitivity	*Specificity*	*Accuracy*
HAM10000 data set	0.88	0.88	0.90
PH2	0.85	0.83	0.89

DOI: https://doi.org/10.54216/JISIoT.080103
Received: May 15, 2022 Accepted: January 23, 2023

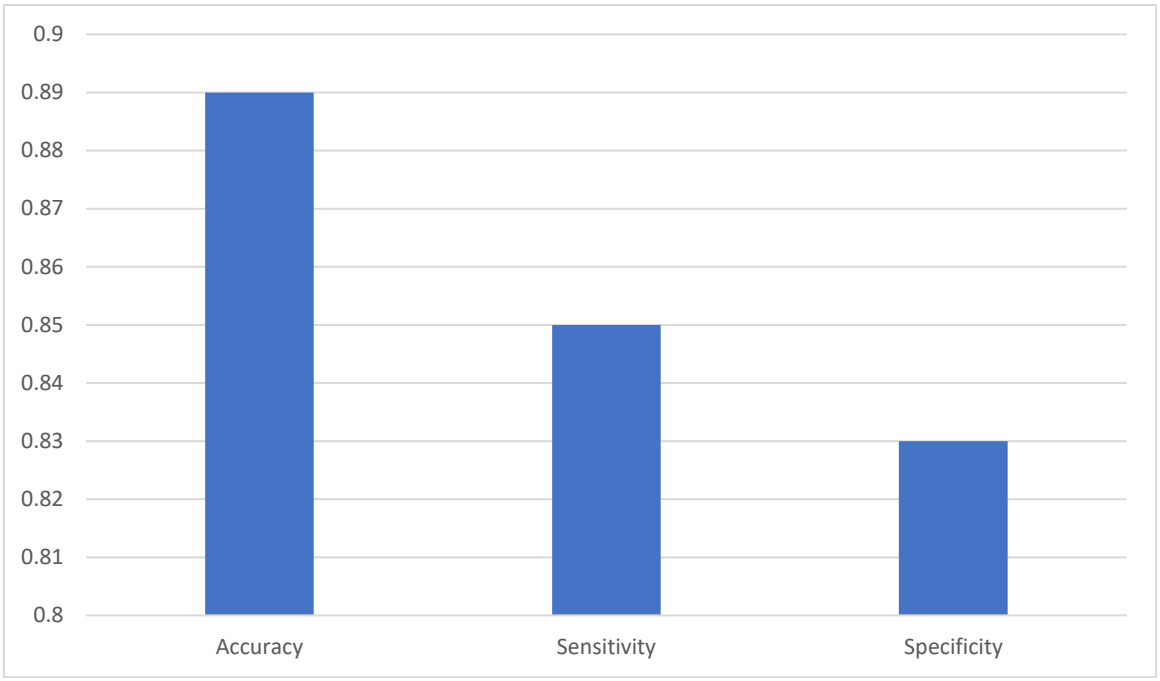

Figure 4: The accuracy of the PH2 dataset.

In this paper, a comparative study between NCMC and FCMC is applied to show the more suitable accuracy. Figure 3 shows the accuracy of both algorithms. From figure 5, the NCMC has the highest accuracy than the FCMC. Therefore, the NCMC is superior to the FCMC.

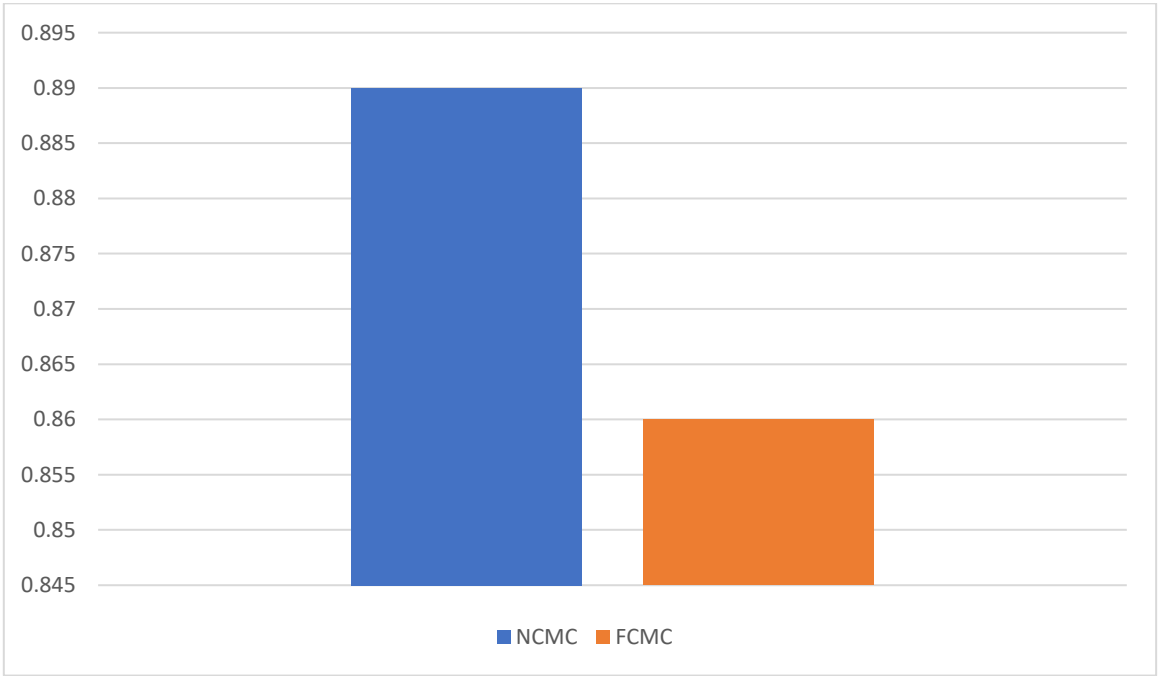

Figure 5: The accuracy of both NCMC and FCMC.

4. Conclusion

It is preferable to diagnose a skin illness as early as possible before it develops into a condition that threatens one's life. As a result, the study that is being presented is an effort to reliably identify early indications of three different forms of skin cancer utilizing procedures that are based on computers. The NCMC classification system is used in this study to categorize different types of skin cancer.

NCMC was created dependent on the NS theory and was meant to manage these drawbacks of the old partition procedures. NCMC was designed to solve these shortcomings of traditional dividing

DOI: https://doi.org/10.54216/JISIoT.080103

Received: May 15, 2022 Accepted: January 23, 2023

methods. It then rebuilt the grouping goal function by making use of NS theory, which stipulates that, the truth (A), the falsity (C), and the indeterminacy (B) for every dataset should be specified in the neutrosophic set. In fuzzy clustering techniques, A is regarded to represent the membership degree. B and C, on the other hand, are used to describe an ambiguous group and an outsider group, correspondingly, for every piece of record. The precision of the method is somewhere near 90% when using the HAM10000 and PH2 dermatoscopic picture datasets.

References

[1] A. G. C. Pacheco and R. A. Krohling, "The impact of patient clinical information on automated skin cancer detection," *Computers in biology and medicine*, vol. 116, p. 103545, 2020.

[2] M. A. Kadampur and S. Al Riyaee, "Skin cancer detection: Applying a deep learning based model driven architecture in the cloud for classifying dermal cell images," *Informatics in Medicine Unlocked*, vol. 18, p. 100282, 2020.

[3] D. N. H. Thanh, V. B. S. Prasath, L. M. Hieu, and N. N. Hien, "Melanoma skin cancer detection method based on adaptive principal curvature, color normalization and feature extraction with the ABCD rule," *Journal of Digital Imaging*, vol. 33, pp. 574–585, 2020.

[4] F. W. Kong, C. Horsham, A. Ngoo, H. P. Soyer, and M. Janda, "Review of smartphone mobile applications for skin cancer detection: what are the changes in availability, functionality, and costs to users over time?" *International Journal of Dermatology*, vol. 60, no. 3, pp. 289–308, 2021.

[5] O. T. Jones *et al.*, "Artificial intelligence and machine learning algorithms for early detection of skin cancer in the community and primary care settings: a systematic review," *The Lancet Digital Health*, vol. 4, no. 6, pp. e466–e476, 2022.

[6] H. Nahata and S. P. Singh, "Deep learning solutions for skin cancer detection and diagnosis," *Machine Learning with Health Care Perspective: Machine Learning and Healthcare*, pp. 159–182, 2020.

[7] M. Kumar, M. Alshehri, R. AlGhamdi, P. Sharma, and V. Deep, "A de-ann inspired skin cancer detection approach using fuzzy c-means clustering," *Mobile Networks and Applications*, vol. 25, no. 4, pp. 1319–1329, 2020.

[8] M. Dildar *et al.*, "Skin cancer detection: a review using deep learning techniques," *International journal of environmental research and public health*, vol. 18, no. 10, p. 5479, 2021.

[9] R. Ashraf *et al.*, "Region-of-interest based transfer learning assisted framework for skin cancer detection," *IEEE Access*, vol. 8, pp. 147858–147871, 2020.

[10] X. Dai, I. Spasić, B. Meyer, S. Chapman, and F. Andres, "Machine learning on mobile: An on-device inference app for skin cancer detection," in *2019 fourth international conference on fog and mobile edge computing (FMEC)*, 2019, pp. 301–305.

[11] Nechirvan Asaad Zebari , Mehmet Emin Tenekeci, Support System Based Computer-Aided Detection for Skin Cancer: A Review, Fusion: Practice and Applications, Vol. 7 , No. 1, 30-40, 2022

[12] Fatma Taher , Ahmed Abdelaziz, Neutrosophic C-Means Clustering with Optimal Machine Learning Enabled Skin Lesion Segmentation and Classification, International Journal of Neutrosophic Science, Vol. 19, No. 1, 177-187, 2022

[13] A. Ameri, "A deep learning approach to skin cancer detection in dermoscopy images," *Journal of Biomedical Physics and Engineering*, vol. 10, no. 6, pp. 801–806, 2020.

[14] L. Wei, K. Ding, and H. Hu, "Automatic skin cancer detection in dermoscopy images based on ensemble lightweight deep learning network," *IEEE Access*, vol. 8, pp. 99633–99647, 2020.

[15] A. Khamparia, P. K. Singh, P. Rani, D. Samanta, A. Khanna, and B. Bhushan, "An internet of health things-driven deep learning framework for detection and classification of skin cancer using transfer learning," *Transactions on Emerging Telecommunications Technologies*, vol. 32, no. 7, p. e3963, 2021.

[16] R. Mohakud and R. Dash, "Designing a grey wolf optimization based hyper-parameter optimized convolutional neural network classifier for skin cancer detection," *Journal of King Saud University-Computer and Information Sciences*, vol. 34, no. 8, pp. 6280–6291, 2022.

[17] A. Murugan, S. A. H. Nair, and K. P. Kumar, "Detection of skin cancer using SVM, random forest and kNN classifiers," *Journal of medical systems*, vol. 43, no. 8, pp. 1–9, 2019.

[18] Y. Guo and A. Sengur, "NCM: Neutrosophic c-means clustering algorithm," *Pattern Recognition*, vol. 48, no. 8, pp. 2710–2724, 2015.

[19] Y. Akbulut, A. Şengür, Y. Guo, and K. Polat, "KNCM: Kernel neutrosophic c-means clustering," *Applied Soft Computing*, vol. 52, pp. 714–724, 2017.

[20] Y. Guo, R. Xia, A. Şengür, and K. Polat, "A novel image segmentation approach based on neutrosophic c-means clustering and indeterminacy filtering," *Neural Computing and Applications*, vol. 28, no. 10, pp. 3009–3019, 2017.

[21] S. Askari, "Fuzzy C-Means clustering algorithm for data with unequal cluster sizes and contaminated with

DOI: https://doi.org/10.54216/JISIoT.080103
Received: May 15, 2022 Accepted: January 23, 2023

noise and outliers: Review and development," *Expert Systems with Applications*, vol. 165, p. 113856, 2021.

[22] C. L. Chowdhary, M. Mittal, P. A. Pattanaik, and Z. Marszalek, "An efficient segmentation and classification system in medical images using intuitionist possibilistic fuzzy C-mean clustering and fuzzy SVM algorithm," *Sensors*, vol. 20, no. 14, p. 3903, 2020.

[23] P. K. Mishro, S. Agrawal, R. Panda, and A. Abraham, "A novel type-2 fuzzy C-means clustering for brain MR image segmentation," *IEEE Transactions on Cybernetics*, vol. 51, no. 8, pp. 3901–3912, 2020.

[24] R. Rout, P. Parida, Y. Alotaibi, S. Alghamdi, and O. I. Khalaf, "Skin lesion extraction using multiscale morphological local variance reconstruction based watershed transform and fast fuzzy C-means clustering," *Symmetry*, vol. 13, no. 11, p. 2085, 2021.

[25] Y. Guo and A. Sengur, "NECM: Neutrosophic evidential c-means clustering algorithm," *Neural Computing and Applications*, vol. 26, pp. 561–571, 2015.

[26] B. Ji, X. Hu, F. Ding, Y. Ji, and H. Gao, "An effective color image segmentation approach using superpixel-neutrosophic C-means clustering and gradient-structural similarity," *Optik*, vol. 260, p. 169039, 2022.

[27] A. M. Anter, A. E. Hassanien, M. A. A. ElSoud, and M. F. Tolba, "Neutrosophic sets and fuzzy c-means clustering for improving ct liver image segmentation," in *Proceedings of the Fifth International Conference on Innovations in Bio-Inspired Computing and Applications IBICA 2014*, 2014, pp. 193–203.

[28] M. K. Alsmadi, "A hybrid Fuzzy C-Means and Neutrosophic for jaw lesions segmentation," *Ain Shams Engineering Journal*, vol. 9, no. 4, pp. 697–706, 2018.

[29] Y. Guo and A. Sengur, "A novel color image segmentation approach based on neutrosophic set and modified fuzzy c-means," *Circuits, Systems, and Signal Processing*, vol. 32, pp. 1699–1723, 2013.

[30] H. D. Cheng, Y. Guo, and Y. Zhang, "A novel image segmentation approach based on neutrosophic set and improved fuzzy c-means algorithm," *New Mathematics and Natural Computation*, vol. 7, no. 01, pp. 155–171, 2011.

[31] A. S. Ashour, Y. Guo, E. Kucukkulahli, P. Erdogmus, and K. Polat, "A hybrid dermoscopy images segmentation approach based on neutrosophic clustering and histogram estimation," *Applied Soft Computing*, vol. 69, pp. 426–434, 2018.

[32] Y. Guo and H.-D. Cheng, "New neutrosophic approach to image segmentation," *Pattern Recognition*, vol. 42, no. 5, pp. 587–595, 2009.

[33] R. Barona and E. A. M. Anita, "Optimal cryptography scheme and efficient neutrosophic C-means clustering for anomaly detection in the cloud environment," *Journal of Circuits, Systems, and Computers*, vol. 30, no. 05, p. 2150084, 2021.

[34] M. N. Qureshi and M. V. Ahamad, "An improved method for image segmentation using K-means clustering with neutrosophic logic," *Procedia computer science*, vol. 132, pp. 534–540, 2018.

[35] A. M. Anter and A. E. Hassenian, "CT liver tumor segmentation hybrid approach using neutrosophic sets, fast fuzzy c-means and adaptive watershed algorithm," *Artificial intelligence in medicine*, vol. 97, pp. 105–117, 2019.

[36] Z. Lu, Y. Qiu, and T. Zhan, "Neutrosophic C-means clustering with local information and noise distance-based kernel metric image segmentation," *Journal of Visual Communication and Image Representation*, vol. 58, pp. 269–276, 2019.

[37] D. S. Irene and T. Sethukarasi, "Efficient Kernel Extreme Learning Machine and Neutrosophic C-means-based Attribute Weighting Method for Medical Data Classification," *Journal of Circuits, Systems, and Computers*, vol. 29, no. 16, p. 2050260, 2020.

[38] F. Zamani, M. H. Olyaee, and A. Khanteymoori, "NCMHap: a novel method for haplotype reconstruction based on Neutrosophic c-means clustering," *BMC bioinformatics*, vol. 21, no. 1, pp. 1–15, 2020.

DOI: https://doi.org/10.54216/JISIoT.080103
Received: May 15, 2022 Accepted: January 23, 2023